

Search ORNL DAAC

Q Search

DAAC Home > Get Data > NASA Projects > Arctic-Boreal Vulnerability Experiment (ABOVE) > User guide

## MODIS-derived Annual Vegetation Resilience, 2000-2019

### Get Data

Documentation Revision Date: 2024-09-12

Dataset Version: 1

### Summary

This dataset provides estimates of vegetation resilience in the Arctic Boreal Vulnerability Experiment (ABOVE) core domain at annual time steps for 2000-2019 and at 300-m spatial resolution. Vegetation resilience is defined as the recovery rate from deviations, due to climate perturbations or disturbances, to the equilibrium state. It is quantified as the negative temporal lag-1 autocorrelation of Enhanced Vegetation Index (EVI). Using a time series of MODIS EVI, the vegetation resilience was estimated using a Bayesian dynamic linear model. The mapped vegetation resilience was derived from Terra EVI products (MOD13Q1v061) across 175 ABOVE B grid tiles over the ABOVE core domain. The estimated mean resilience, upper boundary, and lower boundary results are provided for each tile in cloud optimized GeoTIFF (COG) format.

This dataset contains 525 cloud optimized GeoTIFF (.tif) files. There are three files for each ABOVE tile.

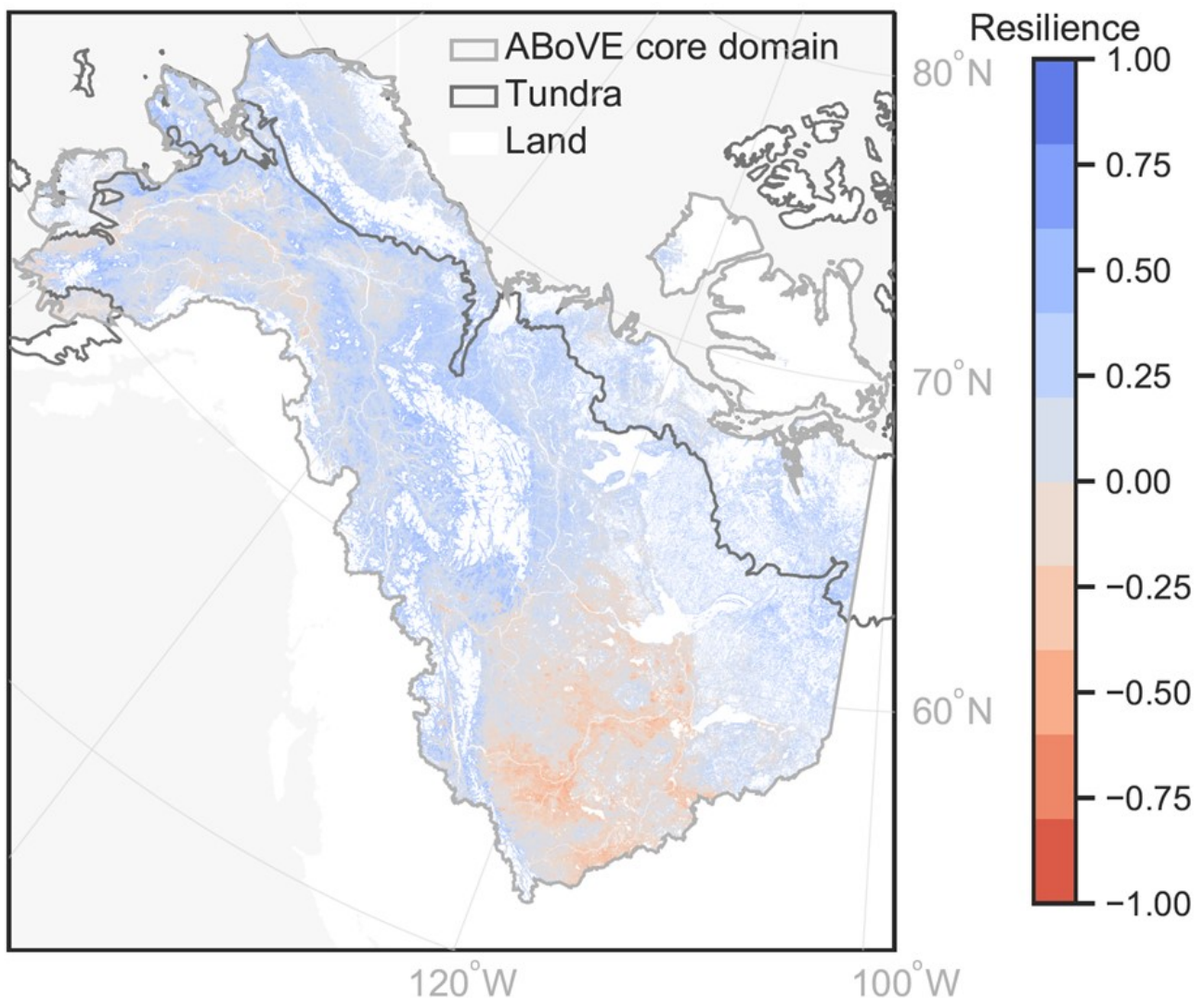


Figure 1. The map of vegetation resilience for the year 2019 in the ABOVE core domain.

# Citation

Zhang, Y., and Y. Liu. 2024. MODIS-derived Annual Vegetation Resilience, 2000-2019. ORNL DAAC, Oak Ridge, Tennessee, USA. <https://doi.org/10.3334/ORNLDAAC/2374>

## Table of Contents

1. Dataset Overview
2. Data Characteristics
3. Application and Derivation
4. Quality Assessment
5. Data Acquisition, Materials, and Methods
6. Data Access
7. References

## 1. Dataset Overview

This dataset provides estimates of vegetation resilience in the Arctic Boreal Vulnerability Experiment (ABoVE) core domain at annual time steps for 2000-2019 and at 300-m spatial resolution. Vegetation resilience is defined as the recovery rate from deviations, due to climate perturbations or disturbances, to the equilibrium state. It is quantified as the negative temporal lag-1 autocorrelation of Enhanced Vegetation Index (EVI). Using a time series of MODIS EVI, the vegetation resilience was estimated using a Bayesian dynamic linear model. The mapped vegetation resilience was derived from Terra EVI products (MOD13Q1v061) across 175 ABoVE B grid tiles over the ABoVE core domain. The estimated mean resilience, upper boundary, and lower boundary results are provided for each tile.

**Project:** [ABoVE](#)

The Arctic-Boreal Vulnerability Experiment (ABoVE) is a NASA Terrestrial Ecology Program field campaign being conducted in Alaska and western Canada, for 8 to 10 years, starting in 2015. Research for ABoVE links field-based, process-level studies with geospatial data products derived from airborne and satellite sensors, providing a foundation for improving the analysis, and modeling capabilities needed to understand and predict ecosystem responses to, and societal implications of, climate change in the Arctic and Boreal regions.

### Related Publication

Zhang, Y., J.A. Wang, L.T. Berner, S.J. Goetz, K. Zhao, and Y. Liu. 2024. Warming and disturbances affect arctic-boreal vegetation resilience across northwestern North America. *Nature Ecology & Evolution* (in review).

### Related Dataset

Loboda, T.V., E.E. Hoy, and M.L. Carroll. 2019. ABoVE: Study Domain and Standard Reference Grids, Version 2. ORNL DAAC, Oak Ridge, Tennessee, USA. <https://doi.org/10.3334/ORNLDAAC/1527>

### Acknowledgement

This research was funded by NASA's Arctic-Boreal Vulnerability Experiment (grant 80NSSC22K1249).

## 2. Data Characteristics

**Spatial Coverage:** Alaska and western Canada

### ABoVE Reference Locations

**Domain:** Core ABoVE

**Spatial Resolution:** 300 m

**Temporal Coverage:** 2000-01-01 to 2019-12-31

**Temporal Resolution:** Annual estimates

**Study Area:** Latitude and longitude are given in decimal degrees.

Site (Region)	Westernmost Longitude	Easternmost Longitude	Northernmost Latitude	Southernmost Latitude
Alaska and Canada	-170.0058	-98.9740	76.2257	50.2590

This dataset contains 525 cloud optimized GeoTIFF (.tif) files. There are three files for each ABoVE tile (Table 1).

The files are named **Bh<XX>v<ZZ>\_ABoVE\_resilience\_<bound>.tif**, where

- <XX> is the horizontal tile location on the ABoVE moderate resolution (B cell) reference grid,
- <ZZ> is the vertical tile location on the ABoVE moderate resolution (B cell) reference grid,
- <bound> designates the "lower\_boundary" or "upper\_boundary" of the mean estimate.

**Table 1.** File descriptions.

File name	Description
Bh<XX>v<ZZ>_ABoVE_resilience.tif	Estimated <i>mean</i> vegetation resilience for tile Bh<XX>v<ZZ>. One band for each year from 2000 to 2019.
Bh<XX>v<ZZ>_ABoVE_resilience_lower_boundary.tif	Estimated <i>lower boundary</i> (mean minus standard deviation) of vegetation resilience for tile Bh<XX>v<ZZ>. One band for each year from 2000 to 2019.

File name	Description
Bh<XX>v<ZZ>_ABoVE_resilience_upper_boundary.tif	Estimated <i>upper boundary</i> (mean plus standard deviation) of vegetation resilience for tile Bh<XX>v<ZZ>. One band for each year from 2000 to 2019.

#### GeoTIFF characteristics

- Coordinate system: NAD 1983 Albers Canada, units = m, (EPSG:102001, the standard ABoVE projection)
- Spatial resolution: 300 m
- Dimensions: 600 rows x 600 columns
- Bands: 20 bands, each corresponds to an annual estimate for 2000 to 2019 (e.g., band 1 is for 2000, band 2 is 2001, etc.)
- Pixel values: vegetation resilience index; unitless values from -1.0 to +1.0.; however, values in lower and upper boundaries may exceed these limits.
- Nodata value: -9999
- Data type: Float32

### 3. Application and Derivation

The dataset provides information on the spatiotemporal pattern of vegetation resilience for the entire ABoVE domain at 300-m resolution over 20 years. These estimates may be used for studies of disturbance-recovery dynamics of vegetation in arctic and boreal biomes.

### 4. Quality Assessment

The uncertainty of the vegetation resilience maps were measured using the standard deviation from the posterior estimates. In this dataset, three files were provided for each ABoVE tile: annual maps of estimated mean vegetation resilience, annual maps of estimated lower boundary of vegetation resilience, and annual maps of estimated upper boundary of vegetation resilience (e.g., Figure 2).

Specifically, at each 16-day time step, the posterior distribution of vegetation resilience was estimated from the prior distribution and likelihood. The 16-day time series of lower/upper boundary of vegetation resilience was defined as the mean minus/plus the standard deviation. The time series of annual vegetation resilience is calculated as the average of 16-day values over June, July and August. Note that the data for the spin-up years 2000-2002 are recommended to be discarded due to large uncertainties.

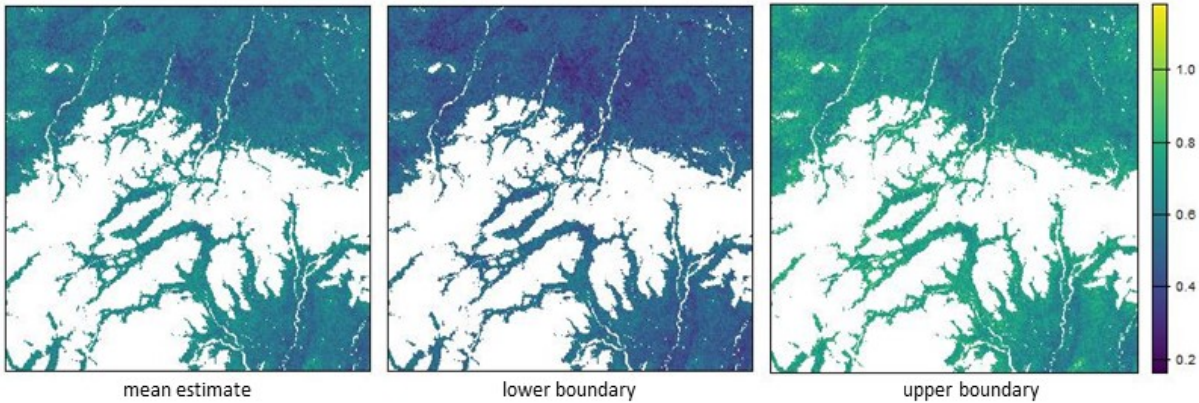


Figure 2. Estimated vegetation resilience for 2009 for ABoVE tile Bh04v05 with lower and upper boundaries of the estimate. Each map is 180 km across.

### 5. Data Acquisition, Materials, and Methods

The 16-day Terra Enhanced Vegetation Index (EVI) products (MOD13Q1v061) from 2000 to 2019 were reprojected into the ABoVE standard Alber's Equal-Area projection (300 m grid, EPSG 102001) and were gridded into 180 km x 180 km ABoVE standard B grid tiles. The vegetation resilience is defined as the recovery rate from deviations, due to climate perturbations or disturbances, to the equilibrium state. Vegetation resilience was quantified as the negative temporal lag-1 autocorrelation of EVI.

The dynamic linear model setup was adapted from Liu et al. (2019) as follows:

$$y_t = \mathbf{F}_t^T \boldsymbol{\theta}_t + v_t \quad (1)$$

$$\boldsymbol{\theta}_t = \mathbf{G} \boldsymbol{\theta}_{t-1} + \mathbf{W}_t \quad (2)$$

where  $y_t$  is the observed EVI at each 16-day time step  $t$  after removing the long-term mean at a pixel. The model disentangles the temporal variation of  $y_t$  into Gaussian observational noise ( $v_t$ ) and three components, i.e., the mean and trend component  $y_{(l,t)}$ , the seasonality component  $y_{(s,t)}$ , and the regression component  $y_{(r,t)}$ , giving  $y_t = y_{(l,t)} + y_{(s,t)} + y_{(r,t)} + v_t$ . Correspondingly,  $\mathbf{F}_t$  (Eq. 3) is a vector consisting of known constants and regressors used to aggregate the three components in the state vector  $\boldsymbol{\theta}_t$  (Eq. 4). Specifically,  $\mathbf{F}_{(l,t)}$  aggregates the mean and trend component  $\boldsymbol{\theta}_{(l,t)}$ , where  $\boldsymbol{\theta}_{(1l,t)}$  and  $\boldsymbol{\theta}_{(l2,t)}$  describe the mean of  $y_{(l,t)}$  and its change from  $t-1$  to  $t$ , respectively, representing the equilibrium state that could adapt to observations to account for shifted equilibrium regime after vegetation changes;  $\mathbf{F}_{(s,t)}$  aggregates the seasonal cycle  $\boldsymbol{\theta}_{(s,t)}$  described by two Fourier components with periods of one year and a half year; and  $\mathbf{F}_{(r,t)}$  includes EVI at the previous time step ( $y_{(t-1)}$ ) and the z-score of mean air temperature ( $T_{(t-1)}$ ), which yields  $y_{(r,t)}$  when multiplied with the regression coefficients  $\boldsymbol{\theta}_{(r,t)} = (\boldsymbol{\theta}_{(lag1,t)}, \boldsymbol{\theta}_{(T(t-1),t)})^T$ . The lag-1 autocorrelation of EVI ( $\boldsymbol{\theta}_{(lag1,t)}$ ) was of particular interest, and  $-\boldsymbol{\theta}_{(lag1,t)}$  was used to measure resilience. The state vector  $\boldsymbol{\theta}_t$  evolves from  $t-1$  to  $t$  based on an evolution matrix  $\mathbf{G} = \text{diag}(\mathbf{G}_l, \mathbf{G}_s, \mathbf{G}_r)$ , where the mean and trend ( $\mathbf{G}_l$ ), seasonality ( $\mathbf{G}_s$ ), and regression  $\mathbf{G}_r$  components consist of

known constants (Eq. 5).

$$\mathbf{F}_t = \underbrace{[1, 0, 1, 0, 1, 0, 0]}_{\mathbf{F}_{l,t}} \underbrace{[y_{t-1}, T_{t-1}]}_{\mathbf{F}_{s,t}} \underbrace{[T_{t-1}]}_{\mathbf{F}_{r,t}}^T \quad (3)$$

$$\boldsymbol{\theta}_t = [\underbrace{\theta_{l1,t}, \theta_{l2,t}}_{\boldsymbol{\theta}_{l,t}}, \underbrace{\theta_{s11,t}, \theta_{s12,t}, \theta_{s21,t}, \theta_{s22,t}}_{\boldsymbol{\theta}_{s,t}}, \underbrace{\theta_{lag1,t}, \theta_{T(t-1),t}}_{\boldsymbol{\theta}_{r,t}}]^T \quad (4)$$

$$\mathbf{G}_l = \begin{bmatrix} 1 & 1 \\ 0 & 1 \end{bmatrix}, \mathbf{G}_s = \begin{bmatrix} \mathbf{G}_{s1} & 0 \\ 0 & \mathbf{G}_{s2} \end{bmatrix}, \mathbf{G}_{si} = \begin{bmatrix} \cos \omega_i & \sin \omega_i \\ -\sin \omega_i & \cos \omega_i \end{bmatrix} \left( i = 1, 2; \omega_1 = \frac{\pi}{6}, \omega_2 = \frac{\pi}{3} \right)$$

$$\mathbf{G}_r = \begin{bmatrix} 1 & 0 \\ 0 & 1 \end{bmatrix} \quad (5)$$

Bayesian inference was used to estimate the resilience embedded in  $\boldsymbol{\theta}_t$  at each time step. Specifically,  $\boldsymbol{\theta}_t$  was assumed to follow a multivariate Gaussian distribution. The same non-informative priors as described in Liu et al. (2019) were used for  $\boldsymbol{\theta}_{(t=0)}$  and the noise. At each time step  $t$ , the posterior distribution of  $\boldsymbol{\theta}_t$ ,  $p(\boldsymbol{\theta}_t | y_1, \dots, y_{(t-1)}, y_t)$  was estimated based on the Bayes theorem by combining the prior of  $\boldsymbol{\theta}_t$ , i.e.,  $p(\boldsymbol{\theta}_t | y_1, \dots, y_{(t-1)})$ , derived from historical observations ( $y_1, \dots, y_{(t-1)}$ ), and the likelihood of observing  $y_t$ , i.e.,  $p(y_t | \boldsymbol{\theta}_t, y_1, \dots, y_{(t-1)})$  (Eq. 6).

$$p(\boldsymbol{\theta}_t | y_1, \dots, y_{t-1}, y_t) \propto p(\boldsymbol{\theta}_t | y_1, \dots, y_{t-1}) p(y_t | \boldsymbol{\theta}_t, y_1, \dots, y_{t-1}). \quad (6)$$

At each 16-day time step, the posterior estimates of  $\boldsymbol{\theta}_t$  is a multivariate t distribution with mean vector  $m$  and covariance  $C$ . The estimated mean and standard deviation of vegetation resilience are the mean and standard deviation of  $-\boldsymbol{\theta}_{(lag1,t)}$ , respectively. The 16-day time series of lower/upper boundary of vegetation resilience is defined as the mean minus/plus the standard deviation. The time series of annual vegetation resilience is calculated as the average of 16-day values over June, July and August.

See Zhang et al. (2024, in review) for further details.

## 6. Data Access

These data are available through the Oak Ridge National Laboratory (ORNL) Distributed Active Archive Center (DAAC).

[MODIS-derived Annual Vegetation Resilience, 2000-2019](#)

Contact for Data Center Access Information:

- E-mail: [uso@daac.ornl.gov](mailto:uso@daac.ornl.gov)
- Telephone: +1 (865) 241-3952

## 7. References

Liu, Y., M. Kumar, G.G. Katul, and A. Porporato. 2019. Reduced resilience as an early warning signal of forest mortality. *Nature Climate Change* 9:880–885. <https://doi.org/10.1038/s41558-019-0583-9>

Loboda, T.V., E.E. Hoy, and M.L. Carroll. 2019. ABoVE: Study Domain and Standard Reference Grids, Version 2. ORNL DAAC, Oak Ridge, Tennessee, USA. <https://doi.org/10.3334/ORNLDAAC/1527>

Zhang, Y., J.A. Wang, L.T. Berner, S.J. Goetz, K. Zhao, and Y. Liu. 2024. Warming and disturbances affect arctic-boreal vegetation resilience across northwestern North America. *Nature Ecology & Evolution* (in review).



[Privacy Policy](#) | [Help](#)



### Home

### About Us

Mission  
Data Use and Citation  
Policy  
User Working Group  
Partners

### Get Data

Science Themes  
NASA Projects  
All Datasets

### Submit Data

Submit Data Form  
Data Scope and  
Acceptance  
Data Authorship Policy  
Data Publication  
Timeline  
Detailed Submission  
Guidelines

### Tools

TESViS  
THREDDS  
SDAT  
Daymet  
Airborne Data Visualizer  
Soil Moisture Visualizer

### Resources

Learning  
Data Management  
News

### Help

Earthdata Forum [↗](#)  
Email Us [✉](#)